The HMX homeodomain protein MLS-2 regulates cleavage orientation, cell proliferation and cell fate specification in the *C. elegans* postembryonic mesoderm

Yuan Jiang, Vanessa Horner and Jun Liu*

Department of Molecular Biology and Genetics, Cornell University, Ithaca, NY 14853, USA
*Author for correspondence (e-mail: JL53@cornell.edu)

Accepted 6 July 2005

Development 132, 4119-4130
Published by The Company of Biologists 2005
doi:10.1242/dev.01967

Summary

The proper formation of a complex multicellular organism requires the precise coordination of many cellular events, including cell proliferation, cell fate specification and differentiation. The *C. elegans* postembryonic mesodermal lineage, the M lineage, allows us to study mechanisms coordinating these events at single cell resolution. We have identified an HMX homeodomain protein MLS-2 in a screen for factors required for M lineage patterning. The MLS-2 protein is present in nuclei of undifferentiated cells in the early M lineage and in a subset of head neurons. In the M lineage, MLS-2 activity appears to be tightly regulated at the fourth round of cell division, coincident with the transition from proliferation to differentiation. A predicted null allele of *mls-2*, *cc615*, causes reduced cell proliferation in the M lineage, whereas a semi-dominant, gain-of-function allele, *tm252*, results in increased cell proliferation. Loss or overexpression of *mls-2* also affects cleavage orientation and cell fate specification in the M lineage. We show that the increased cell proliferation in *mls-2(tm252)* mutants requires CYE-1, a G1 cell cycle regulator. Furthermore, the *C. elegans* Myod homolog HLH-1 acts downstream of *mls-2* to specify M-derived coelomocyte cell fates. Thus MLS-2 functions in a cell type-specific manner to regulate both cell proliferation and cell fate specification.

Key words: *mls-2*, HMX, Nkx5, Homeodomain, *C. elegans*, Mesoderm, Cleavage orientation, Cell proliferation, Cell fate specification, HLH-1, Myod, CYE-1

Introduction

The proper formation of a complex multicellular organism requires the precise coordination of many cellular events, including cell proliferation, cell fate specification and differentiation. The *C. elegans* postembryonic mesodermal lineage, the M lineage, allows us to study how these events are integrated at single cell resolution. The M lineage is derived from a single progenitor cell, the M mesoblast, which is born during embryogenesis but remains mitotically quiescent until the larva hatches (Sulston et al., 1983; Sulston and Horvitz, 1977). During larval development, the M cell undergoes a series of characteristic and reproducible divisions to produce all of the postembryonically derived, non-gonadal mesodermal cells (Sulston and Horvitz, 1977). In hermaphrodite animals, the first four (or five for two cells, M.vlpa and M.vrpa) rounds of cell divisions in the M lineage result in the formation of fourteen striated body wall muscles (BWMs), two non-muscle coelomocytes (CCs) and two sex myoblasts (SMs) (Sulston and Horvitz, 1977) (Fig. 1). The two SMs remain mitotically quiescent while migrating towards the future vulval region. At the vulval region, the two SMs divide three times, each producing four vulval muscles (VMs) and four uterine muscles (UMs; Fig. 1).

Previous studies have identified a number of regulatory factors that function in the proper patterning and fate specification of the M lineage, including the Hox factors MAB-5 and LIN-39, their cofactor CEH-20 (Kenyon, 1986; Harfe et al., 1998b; Liu and Fire, 2000), the *C. elegans* Myod homolog HLH-1, the Twist ortholog HLH-8 (Harfe et al., 1998a; Harfe et al., 1998b; Corsi et al., 2000; Corsi et al., 2002) and the Notch receptor LIN-12 (Greenwald et al., 1983). MAB-5 and LIN-39, together with CEH-20, are crucial for diversification of the M lineage, and they directly activate the expression of HLH-8 (Liu and Fire, 2000). HLH-1 and LIN-12 have been implicated in cell fate decisions between coelomocytes and sex myoblasts (Greenwald et al., 1983; Harfe et al., 1998a). These factors, however, do not account for all of the mechanisms involved in the development of the M lineage.

We have carried out a genetic screen to identify mutations that affect the proper patterning of the M lineage. In this report, we describe one of the genes identified in this screen, *mls-2* (*mesodermal lineage specification-2*). *mls-2* encodes a homeodomain protein of the HMX family, also known as the Nkx5 family (Pollard and Holland, 2000). We report our analysis on the multiple and distinct functions of MLS-2 in the M lineage. We further identify the bHLH transcription factor HLH-1 as a downstream target of MLS-2 in regulating cell fate specification in the M lineage.

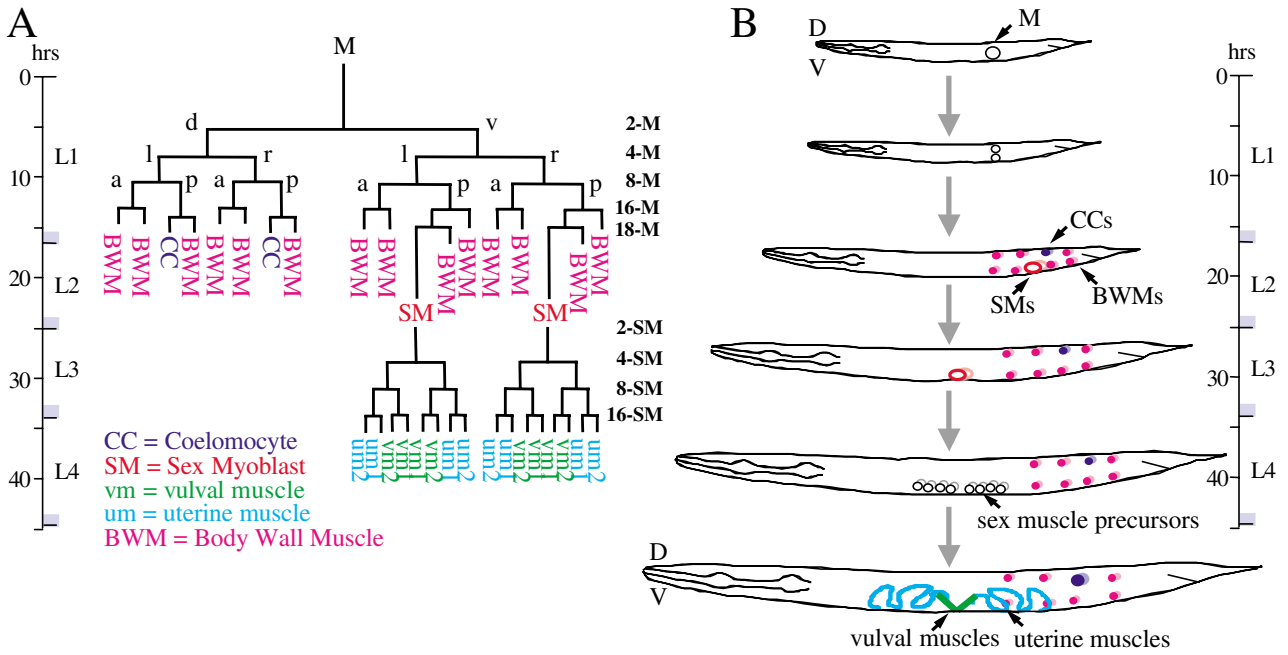

Fig. 1. The *C. elegans* hermaphrodite postembryonic M lineage. Times indicated are hours post-hatching at 25°C. (A) The M lineage with all the differentiated cell types (modified from Sulston and Hovitz, 1977). The corresponding stages referred to in the paper are indicated on the right. (B) A schematic lateral view of the M lineage through larval development. D, dorsal; V, ventral; L, left; R, right; A, anterior; P, posterior.

Materials and methods

C. elegans strains

Strains were manipulated under standard conditions, as described by Brenner (Brenner, 1974). Analyses were performed at 20°C, unless otherwise noted. The following strain was generated for observing the M lineage in *cc615* mutant animals throughout postembryonic development: LW0050 [*ccIs4438(intrinsic CC::gfp)* III; *ayIs2(egl-15::gfp)* IV; *mls-2(cc615) ayIs6(hlh-8::gfp)* X]. The strain LW0081 [*ccIs4438(intrinsic CC::gfp)* III; *ayIs2(egl-15::gfp)* IV; *ayIs6(hlh-8::gfp)* X] was used as the corresponding wild-type control. Additional cell-type-specific reporters for the M lineage were as described in Kostas and Fire (Kostas and Fire, 2002). The M lineage was followed in live animals under a fluorescence stereomicroscope and confirmed using the compound microscope.

Additional strains used in this work were as follows.

LG I: *ayIs4 [egl-17::gfp]* (Burdine et al., 1998); *cye-1(eh10)/dpy-14(e188)* (Brodigan et al., 2003); *dpy-5(e61) cye-1(ar95)/unc-13(e51)* (Seydoux et al., 1993); *lin-6(e1466) dpy-5(e61) I/hT2[qIs48](I;III)* (Wang and Kimble, 2001).

LG II: *hlh-1(cc561ts)* (Harfe et al., 1998a).

LG III: *mab-5(e1239), lin-39(n1760) mab-5(e1239)/dyp-17(e164) unc-32(e189)* (Liu and Fire, 2000); *pha-1(e2123ts)* (Schnabel and Schnabel, 1990).

LG V: *him-5(e1467)* (Hodgkin et al., 1979).

LG X: *hlh-8(nr2061)* (Corsi et al., 2000); *unc-2(e55) lon-2(e678), dpy-8(e130) unc-124(hs10)* (Hecht et al., 1996); *mls-2(tm252)* (gift from Shohei Mitani, Tokyo Women's Medical University School of Medicine, Japan).

Mutagenesis screen and analysis of *mls-2*

PD4666(*ayIs6*) animals carrying an integrated *hlh-8::gfp* reporter that labels all undifferentiated M lineage descendants were mutagenized with ethylmethylsulfonate (EMS). Non-clonal F2 populations were screened using a fluorescence stereomicroscope. Animals with abnormal M lineage patterning were recovered for further analysis. We screened 15,000 haploid genomes and isolated 15 independent mutations with an altered M lineage. One recessive mutation, *cc615*, showed 100% penetrance of M lineage defects and defines the *mls-2* locus. Three-factor mapping using *unc-2(e55) lon-2(e678)* and *dpy-8(e130) unc-124(hs10)*, coupled with snip-SNP mapping (Wicks et al., 2001), placed *mls-2* between C07A12.2 and F43C9.2 on the X chromosome. Among 13 likely candidates of the 40 predicted genes located in this region, RNAi of C39E6.4 in wild-type animals phenocopied the *cc615* M lineage phenotype. Cosmid C39E6 rescued the *cc615* mutant phenotype. The molecular lesions of *cc615* were identified through direct sequencing of PCR fragments encompassing the entire coding region of C39E6.4.

Plasmid constructs and transgenic lines

mls-2 reporter constructs

5.5 kb of the *mls-2* promoter sequence (–5567 to –1), the entire *mls-2* coding region and 2.1 kb of the *mls-2* downstream sequence were amplified through long-range PCR (Expand Long Template PCR system, Roche), using cosmid C39E6 as template. The PCR products were used to generate the following reporter constructs for analyzing the expression pattern of *mls-2*:

pYJ55, 5.5 kb *mls-2p::gfp::mls-2* 3′ UTR;
pYJ59, 5.5 kb *mls-2p::gfp::mls-2::mls-2* 3′ UTR.

Forced expression constructs

pYJ62, *hsp16p::mls-2::mls-2* 3′ UTR;
pYJ63, *hlh-8p::mls-2::mls-2* 3′ UTR;
pYJ86, *hlh-8p::hlh-1::unc-54* 3′ UTR.

Detailed information on all the constructs is available upon request. Plasmid pKM1110 (*cye-1::gfp*) was from Mike Krause (Brodigan et al., 2003). Transgenic lines were generated using the plasmid pRF4 (Mello et al., 1991) or the *pha-1* rescuing plasmid pC1 (Granato et al., 1994) as markers.

Heat-shock experiments

To examine the effects of forced expression of *mls-2* on the M lineage, animals carrying pYJ62[*hsp16p::mls-2::mls-2* 3′ UTR] were stage synchronized with respect to M lineage development using the integrated *hlh-8::gfp*. Animals of the same stage were transferred to the same plate, heat shocked at 37°C for 1 hour and analyzed at different time points after recovery at 20°C. The M lineage phenotype was examined using *hlh-8::gfp, egl-15::gfp* and *CC::gfp* markers, and compared with that of control animals (LW0081) that had undergone the same treatment.

To examine the consequences of forced expression of *mls-2* on other cell types, animals carrying pYJ62 were stage synchronized and heat shocked at 37°C for 30 minutes to 1 hour, every 8 or 12 hours starting from late embryogenesis. The intestinal cells, seam cells and cells in the vulva were examined using *cye-1::gfp*, *egl-17::gfp*, DIC optics and DAPI staining.

RNAi

Plasmids *yk276h9* (gift from Yuji Kohara, National Institute of Genetics, Japan) and pVZ1200 (gift from Mike Krause, NIDDK, NIH, USA) were used as templates for synthesizing dsRNA against *mls-2* and *hlh-1*, respectively, following the protocol of Fire and colleagues (Fire et al., 1998). dsRNA was injected into gravid adults of different genotypes. Progeny of injected animals were scored for larval lethality and M lineage defects. Water-injected animals were used as controls.

Antibodies and immunofluorescence staining

The N terminus of MLS-2 (amino acids 14 to 215) was cloned into pGEX-4T-1 (Smith and Johnson, 1988). Plasmid pYJ67 was transformed into BL21(DE3)pLysS cells. Fusion proteins were first purified under denaturing conditions using Glutathione sepharose 4B beads (Amersham Biosciences) and further purified by SDS-PAGE. Gel slices containing the purified fusion proteins were used to immunize rats (Cocalico Biologicals, PA). The resulting antisera were tested by western blot analyses using bacterially generated GST-MLS-2 fusion proteins. Antibodies were further purified by pre-adsoption with extracts of *mls-2(cc615)* mutant worms at 4°C overnight (Maloof and Kenyon, 1998).

For immunostaining using anti-HLH-1 antibodies, animals were fixed following the protocol of Harfe and colleagues (Harfe et al., 1998a). For all other antibodies, animals were fixed following the protocol of Hurd and Kemphues (Hurd and Kemphues, 2003). The following antibodies were used: preadsorbed rat anti-MLS-2 (CUMC-R6; 1:400 to 1:1000), goat anti-GFP (Rockland Immunochemicals; 1:5000), mouse anti-β-galactosidase (Promega; 1:50) and rabbit anti-HLH-1 (Krause et al., 1990) (gift of M. Krause; 1:400). All secondary antibodies were from Jackson ImmunoResearch Laboratories and were used at a dilution of 1:100 to 1:400. Differential interference contrast and epifluorescence microscopy were performed using a Leica DMRA2 compound microscope. Images were captured by a Hamamatsu Orca-ER camera using the Openlab software (version 3.0.9, Improvision). Subsequent image analysis was performed using Adobe Photoshop 7.0.

Results

mls-2(cc615) mutants display abnormal cleavage orientation, under-proliferation and cell fate transformation in the M lineage

In a screen for mutants with abnormal M lineage patterning (see Materials and methods), we isolated the mutation *cc615*. Animals homozygous for *cc615* were 100% penetrant for their M lineage defects, and exhibited approximately 30% larval and adult lethality. The mutation was completely recessive and showed no evidence of defects from maternal inheritance. We designated the gene corresponding to *cc615* *mls-2* (*mesodermal lineage specification-2*).

We analyzed the M lineage in *cc615* mutants by following post-embryonic development in live animals using molecular markers that label different cell types of the M lineage. Using the *hlh-8::gfp* reporter as a marker for undifferentiated cells in the M lineage (Harfe et al., 1998b), the first defect we observed was abnormal cleavage orientation in *cc615* mutants. In wild-type animals, the M mesoblast always undergoes the first cell division along the dorsoventral axis (Fig. 2A). However, among the 32 *cc615* mutants examined, only 69% divided with this orientation, and the cleavage plane was sometimes tilted (data not shown). In the remaining 31%, the first division of M was oriented in the anteroposterior direction (Fig. 2B). Very rarely, we observed M division along the left-right axis (data not shown). Subsequent cleavage orientations of the M lineage divisions continued to be randomized in *cc615* mutants (Fig. 3B-D). The resulting M descendants were located in the posterior of *cc615* mutant animals in variable patterns (see Fig. 2E as an example), instead of being positioned in four quadrants, as in wild-type animals (Fig. 2D).

In addition to the cleavage orientation defects, *cc615* mutants also exhibited defects in cell proliferation and cell fate specification in the M lineage. In wild-type hermaphrodites, the M mesoblast first undergoes four rounds of cell division to produce 16 descendants expressing *hlh-8::gfp* (Fig. 1). In *cc615* mutant animals, M always completed the first three rounds of cell divisions, generating eight *hlh-8::gfp* expressing cells. However, zero to six of the eight cells divided for a fourth time in *cc615* mutants, yielding a range of 8-14 M lineage descendants (Fig. 2E, Fig. 3B-D). Thus at late L1 stage, *mls-2(cc615)* mutant animals contained a reduced number of M lineage descendants when compared with wild-type animals at the same stage.

After the fourth round of cell division in the wild-type M lineage, two of the 16 cells on the ventral side undergo an extra round of division, with the M lineage producing 14 BWMs, 2 CCs and 2 SMs (Fig. 1). Using Nomarski optics in combination with the *myo-3::gfp* marker and the *intrinsic cc::gfp* marker, which label BWMs and CCs, respectively (Kostas and Fire, 2002), we found that all *cc615* mutants had the correct number of embryonically derived CCs and BWMs, but lacked M-derived CCs, and most or all M-derived BWMs (Table 1, Fig. 2J,K, Fig. 3B-D). Instead, *cc615* mutants contained more than two M-derived cells (three to nine cells) that behaved like SMs (Table 1, Fig. 3B-D). These SM-like cells were enlarged, expressed *hlh-8::gfp* and migrated toward the vulva to various degrees (Fig. 2H). They divided two to three times to generate multiple sex muscle precursors that differentiated into appropriate vulval and uterine muscles, as verified by a number of sex muscle-specific GFP markers, including *egl-15::gfp*, *arg-1::gfp* and *NdE box::gfp* (Fig. 2K). The presence of vulval muscles was also confirmed by observing the light diffraction of the muscles using polarized light. Among the SM-like cells in *cc615* mutants, two cells always migrated to the ventral side around the vulva and generated the correct number of sex muscles that attached properly and appeared functional. *cc615* mutant animals did not have any egg-laying defects (data not shown). Thus, *cc615* mutant animals produce extra SMs at the expense of M lineage-derived CCs and BWMs.

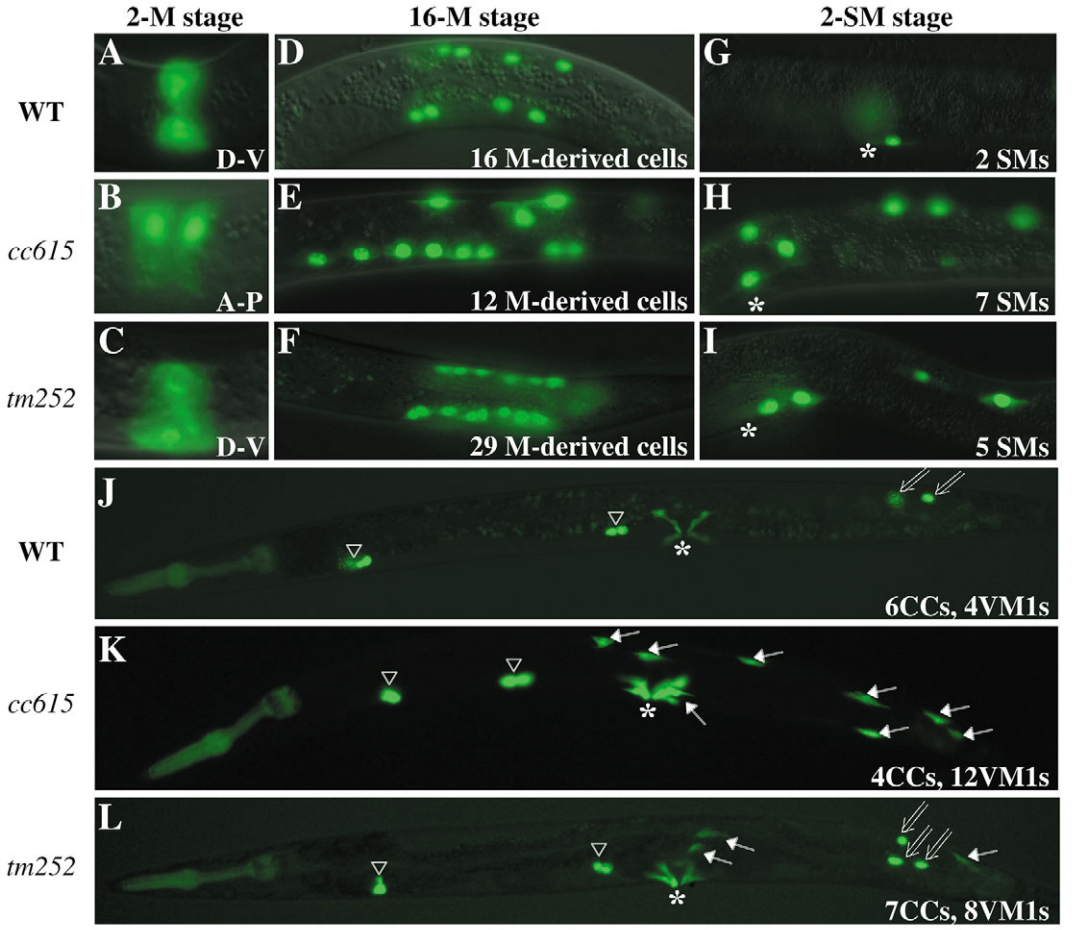

Fig. 2. The M lineage phenotypes of *cc615* and *tm252* mutants. All images are lateral views of animals with anterior to the left and dorsal up; asterisk indicates position of the vulva. The number of M-derived precursors or products in each panel indicates the total number of corresponding cell types in the particular mutant. (A-I) The M lineage of wild-type (A,D,G), *cc615* (B,E,H) and *tm252* (C,F,I) hermaphrodites as visualized by *hlh-8::gfp*. (A-C) Cleavage orientation of M showing the positions of the two M daughters. (D-F) The M lineage undifferentiated products at the late L1 stage. (D) 16 M-derived cells are present in wild-type animals, with eight visible in the focal plane shown. (E) A *cc615* mutant animal with 12 M-derived cells, 11 of them are visible in the focal plane shown because of defects in cleavage orientations. (F) A *tm252* mutant animal with 29 M-derived cells, 14 of them visible in the focal plane shown. (G-I) Positions of SMs at late L2 stage. (G) Two SMs (one out of focus) in wild-type animals at the future vulval region. (H,I) Multiple SMs (one focal plane shown) in *cc615* (H) and *tm252* (I) mutants, with some SMs exhibiting migration defects. (J-L) Differentiated M lineage products in adult wild-type (J), *cc615* (K) and *tm252* (L) hermaphrodites. Arrow, VM1 visualized by *egl-15::gfp*; open arrowhead and double-line arrow, embryonically-derived CCs and M-derived CCs, respectively, as visualized by *intrinsic CC::gfp*. (J) A wild-type animal with two dorsal M-derived CCs and four VM1s. (K) A *cc615* animal with no M-derived CCs and extra VM1s (some do not migrate properly). (L) A *tm252* animal with extra VM1s and CCs.

mls-2 encodes a homeodomain protein of the HMX family

We mapped *mls-2* to an interval between C07A12.2 and F43C9.2 on the left arm of chromosome X. This region covers 40 predicted genes. RNAi injection of one of them, C39E6.4, resulted in close to 100% penetrance of M lineage defects similar to those observed in *mls-2(cc615)* mutants, suggesting that C39E6.4 was *mls-2* (see Materials and methods). We rescued the *cc615* mutant phenotypes with a DNA fragment containing the genomic region of C39E6.4 and identified two molecular lesions in the coding region of C39E6.4 in *cc615* mutants (Fig. 4A). The first lesion is a nonsense mutation at residue 28 (CAA to TAA, Gln to Ochre Stop) and the second lesion is a mis-sense mutation at residue 55 (GAG to GAT, Glu to Asp). The presence of the premature stop codon suggests that *cc615* is likely a null allele. Additional evidence that *cc615* is a null mutation is provided by the immunostaining results discussed below (Fig. 4A).

The predicted MLS-2 protein is 341 amino acids in length and contains a homeodomain between residues 201 and 260 (Fig. 4A,B). This homeodomain is most similar to that of the Nkx5 family of homeodomain proteins, also known as the HMX family. The HMX gene family is present in many organisms from sea urchins to humans (Adamska et al., 2000; Adamska et al., 2001; Bober et al., 1994; Deitcher et al., 1994; Herbrand et al., 1998; Martinez and Davidson, 1997; Rinkwitz-Brandt et al., 1995; Rinkwitz-Brandt et al., 1996; Shaw et al., 2003; Stadler et al., 1992; Stadler et al., 1995; Stadler and Solursh, 1994; Wang et al., 1990; Wang et al., 2000; Yoshiura et al., 1998). HMX proteins share homology in the

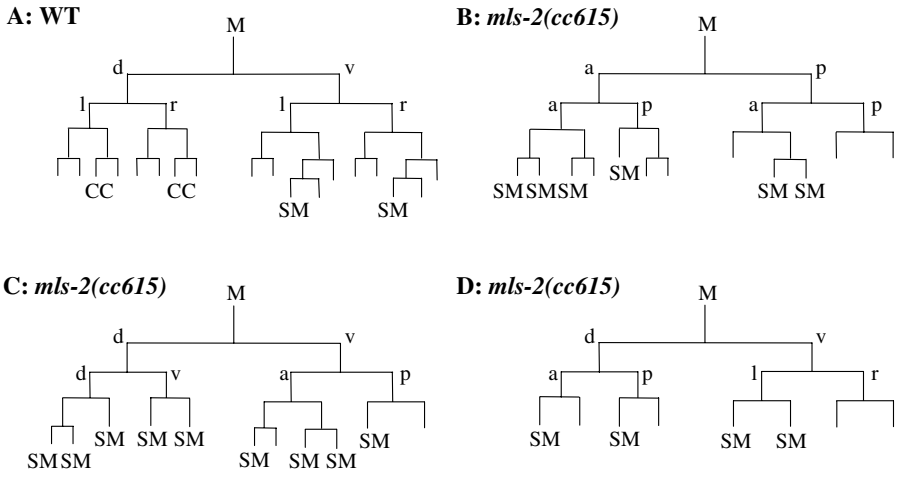

Fig. 3. The early M lineage in wild-type and *mls-2(cc615)* animals. (A-D) The M lineage of wild type (A) and sample animals of *cc615* mutants (B-D). The M lineage was followed from L1 to L4 stage in 15 wild-type and 32 *cc615* mutant animals. Orientations of the first two divisions are indicated to show randomized cleavage orientations in *cc615* mutants. All *cc615* mutants exhibited reduced proliferation after the 8-M stage (B-D). We consistently observed loss of both M-derived CCs and supernumerary SM-like cells in *cc615* mutants. Cells that may adopt the BWM fate or fail to express any M lineage markers are unmarked.

homeodomain and in two additional regions immediately C-terminal to the homeodomain (Wang et al., 2000; Yoshiura et al., 1998). Alignment of MLS-2 with other HMX family members, and with a *C. elegans* Nkx2.5 homolog, CEH-22 (Okkema and Fire, 1994), is shown in Fig. 4B,C. Similarity between MLS-2 and other HMX proteins is limited to the homeodomain region. MLS-2 is most similar to the chick HMX protein SOHo1 (Deitcher et al., 1994).

MLS-2 protein is localized in the nuclei of early M lineage cells and a subset of head neurons

To begin to determine where MLS-2 functions, we examined the temporal and spatial expression of MLS-2. We generated a translational *mls-2p::gfp::mls-2::mls-2* 3′ UTR fusion construct that fully rescued the M lineage defects of *cc615* mutants (Fig. 4A). We also generated rat polyclonal anti-MLS-2 antibodies for immunohistochemical staining to detect the endogenous MLS-2 protein (Fig. 4A). The antibodies specifically recognized a protein of the predicted size for MLS-2 (38 kDa) on western blots using worm extracts (data not shown), and failed to detect any signal in *cc615* homozygous mutants (Fig. 5I,J).

The GFP::MLS-2 fusion construct and antibody staining showed identical expression patterns (Fig. 5A-H). Expression of MLS-2 was first detectable in one or two cells in embryos at the 50-cell stage (data not shown) and is localized in the nucleus. MLS-2 continued to be expressed in proliferating cells that are primarily located at the anterior of the embryo and are presumably derived from the AB lineage (Fig. 5A-D). During morphogenesis, this expression became restricted to a small subset of head neuronal precursors. Expression persisted in six head neurons during postembryonic development (Fig. 5E,F). We also observed GFP::MLS-2 expression in unidentified cells near the vulva at the L2 and L3 stages (data not shown).

To characterize the M lineage expression pattern of *mls-2*, we performed double-labeling experiments using anti-MLS-2 antibodies and the M lineage-specific *hlh-8::gfp* or *hlh-8::lacZ* markers (Harfe et al., 1998b). *mls-2* expression in the M lineage was first detectable in the M mesoblast (Fig. 5P-R), and was retained during the first three rounds of cell divisions, such that *mls-2* expression was still detectable in eight M descendants (designated 8-M stage, n>200, Fig. 5M,N). However, after one more round of cell division (at the 16-M stage), no MLS-2 signal was detected either by anti-MLS-2 antibodies or by the *gfp::mls-2* fusion construct (n>50,

Table 1. Differentiated M lineage descendants in *mls-2* and *cye-1* mutant animals

Genotype	Number of M-derived BWMs (*myo-3::gfp*)	Number of M-derived CCs (*intrinsic CC:gfp*)	Number of SMs (*hlh-8::gfp*)	Number of VM1s (*egl-15::gfp*)
Wild type	14 (n=3)	2 (100%) n>100	2 (n>100)	4 (n>100)
cc615/cc615	0-3 (n=16)	0 (100%) n>100	3-9 (n=32)	6-14 (n=50)
*tm252/tm252**	17-25 (n=6)	0 (32%) 1-2 (51%) n=115 3-4 (17%)	2-9 (n=29)	4-12 (n=43)
*tm252/+**	N/A	0 (48%) 1-2 (47%) n=62 3 (5%)	2-5 (n=21)	4-8 (n=62)
eh10/eh10	N/A	0 (19%) 1 (81%) n=63	1-3 (n>100)	2-5 (n>100)†
eh10/eh10; tm252/ tm252	N/A	0 (90%) 1 (10%) n=85	1-3 (n>100)	2-5 (n>100)†

*4% of *tm252/tm252* animals (n=115) and 18% of *tm252/+* animals (n=62) were completely wild type with regard to the M lineage.
†Some *egl-15::gfp*-positive cells lacked the morphology of normal vulval muscles.

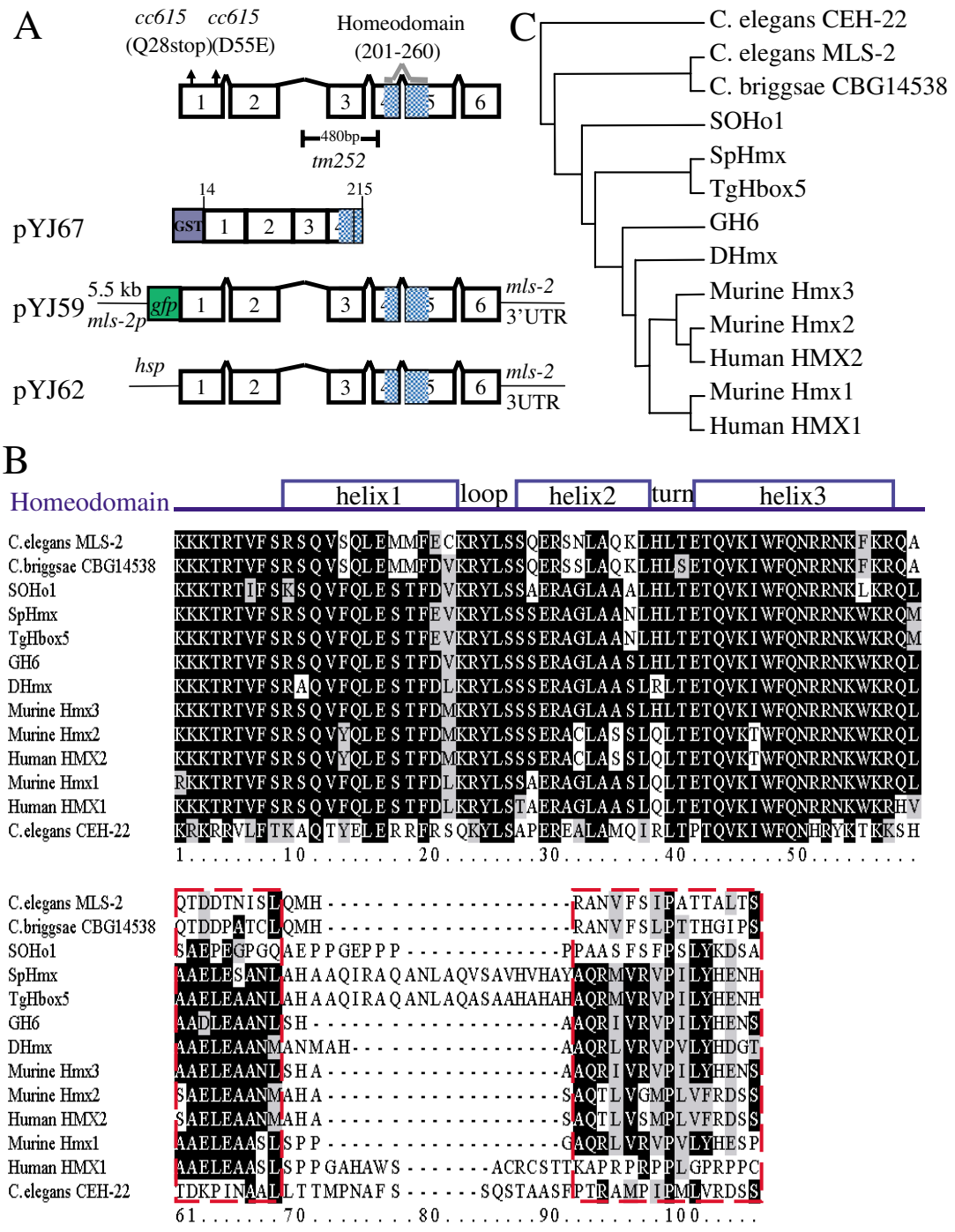

Fig. 4. *mls-2* encodes a homeodomain protein of the HMX family. (A) *mls-2* gene structure and constructs. The upper diagram represents the six exons of the *mls-2* genomic sequence, with the molecular lesions in *cc615* and *tm252* indicated. Shaded areas represent the homeodomain. The lower diagram depicts various fusion constructs used in this work (see Materials and methods). Both pYJ59 and pYJ62 were able to rescue the *mls-2(cc615)* mutant phenotypes. (B) A Clustal W sequence alignment of MLS-2, other HMX (Nkx5) family homeodomain proteins and the *C. elegans* Nkx2.5 homolog CEH-22. Only residues within the homeodomain (residues 1-60) and two additional domains (in dashed boxes) immediately after the homeodomain were aligned. The proteins share no similarity outside this compared region. Identical amino acids are in white letters against black background. Similar amino acids are in black letters against gray background. The alignment is shown for CeMLS-2 (this work), *C. briggsae* CBG14538 (WormBase), SOHo1 (chicken) (Deitcher et al., 1994), SpHmx (sea urchin) (Martinez and Davidson, 1997), TgHbox5 (sea urchin) (Wang et al., 1990), GH6 (chicken) (Stadler et al., 1994), DHmx (*Drosophila*) (Wang et al., 2000), murine Hmx3 (Nkx-5.1) (Bober et al., 1994), murine Hmx2 (Nkx-5.2) (Bober et al., 1994), human HMX2 (Wang et al., 2000), murine Hmx1 (Yoshiura et al., 1998), human HMX1 (H6) (Stadler et al., 1992) and CEH-22 (Okkema and Fire, 1994). (C) A phylogenetic tree of the HMX family generated using the neighbor-joining method of Clustal W. The tree is rooted with CEH-22 in TreeView version 1.6.6 (Page, 1996). Only the homeodomain and the two additional conserved domains immediately after the homeodomain (as shown in B) were used in the analysis.

data not shown). Although we cannot rule out the possibility that a low level of MLS-2 protein is present after the 8-M stage, the loss of MLS-2 signal at the 16-M stage appears to be due to the instability of the MLS-2 protein, because the *mls-2* promoter is still active in M lineage descendants after the fourth round of cell division, as detected by a transcriptional *mls-2p::gfp::mls-2* 3′ UTR construct (Fig. 5O). Neither the *mls-2* promoter activity nor the MLS-2 protein was detected in the SM lineage (Fig. 5S-U) or the differentiated BWMs and CCs (data not shown). Thus *mls-2* is expressed in the proliferating cells of the early M lineage (Fig. 5V).

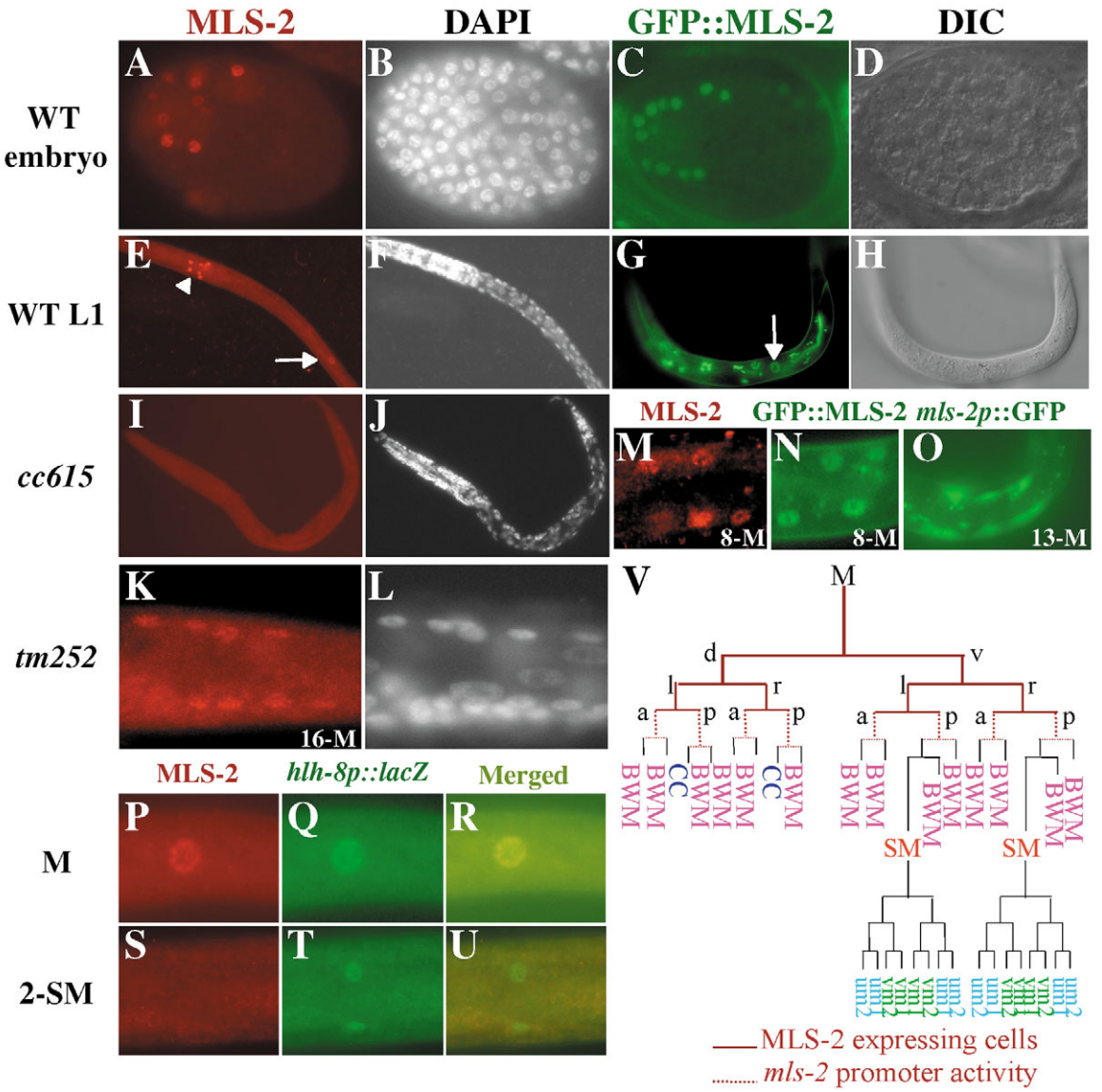

Fig. 5. Expression pattern of *mls-2* in wild-type, *cc615* and *tm252* hermaphrodites. (A,B,E,F,M) Wild-type embryos (A,B) and L1 larvae (E,F,M) stained with anti-MLS-2 antibody (A,E,M) or DAPI (B,F). (C,G,N) Expression pattern of a functional GFP::MLS-2 fusion in wild-type embryos (C) and early L1 larvae (G,N). (D,H) Corresponding DIC images for panels C and G. Nuclear localized MLS-2 protein was seen in a subset of cells during embryogenesis (A,C), in six head neurons (arrowhead in E; the neuronal signal was out of focus in G), in the M mesoblast (arrows in E and G) and in the eight M descendants (M,N; only four cells visible in this focal plane). No MLS-2 protein was detected after the 8-M stage (n>50). Note that the other signals shown in G are due to gut autofluorescence. (I-L) *cc615* (I,J) and *tm252* (K,L) L1 larvae stained with anti-MLS-2 antibody (I,K) or DAPI (J,L). (I) No MLS-2 staining was detected in *cc615* mutants (n>50). (K) The MLS-2(gf) protein in *tm252* mutants was detected in the 16 M descendants (eight visible in this focal plane) and the head neurons (data not shown). (O) GFP signal from a *mls-2p::gfp* transgene in an animal with 13 M descendants (six GFP-expressing cells visible in the focal plane shown). The GFP signal is primarily cytoplasmic. (P-U) Transgenic animals carrying an integrated *hlh-8p::lacZ* reporter were double-stained with both anti-MLS-2 (P,S) and anti-β-galactosidase (Q,T) antibodies. (R,U) Merged images. MLS-2 protein was detected in the M mesoblast (P-R), but not in the SMs (S-U). (V) Summary of *mls-2* expression pattern in the M lineage. The wild-type M lineage with overlay of *mls-2* expression highlighted in red. Solid red lines indicate *mls-2* expression detected by both GFP::MLS-2 and anti-MLS-2 antibodies; dashed red lines indicate *mls-2* expression detected only by a transcriptional *mls-2p::gfp* reporter.

Table 2. Effect of forced expression of MLS-2 on the M lineage

Phenotypes (number of M-derived CCs and VM1s)	Overexpressing *mls-2* in the early M lineage		Ectopically expressing *mls-2* in the SM lineage	
	Wild-type control (*n*=65)	*hsp::mls-2* (*n*=35)	Wild-type control (*n*=35)	*hsp::mls-2* (*n*=30)
0 CCs, >4 VM1s	0	23%	0	0
1 CCs, >4 VM1s	0	9%	0	0
2 CCs, 4 VM1s	100%	14%	100%	27%
2 CCs, >4 VM1s	0	28%	0	73%
3-5 CCs, ⩾4 VM1s	0	26%	0	0

A gain-of-function *mls-2* mutation, *tm252*, causes over-proliferation and abnormal cell fate specification in the M lineage

A deletion allele of *mls-2*, *tm252*, was generated by Shohei Mitani's laboratory. *tm252* contains a deletion of 480 bp of the *mls-2* genomic sequences (from the middle of intron 2 to the beginning portion of exon 4) and an insertion of a T after the deletion (Fig. 4A). We out-crossed the *tm252* mutants and analyzed their M lineage phenotypes. Unlike *cc615*, *tm252* did not affect cleavage orientation in the M lineage (Fig. 2C). However, extra cell divisions occurred after four rounds of proper cell division in more than 80% of *tm252* mutant animals scored (*n*>50), resulting in more than 18 *hlh-8::gfp* expressing cells in the early M lineage (see Fig. 2F for an example). We also observed extra M-derived BWMs and SMs, as well as variable numbers of CCs in *tm252* mutants (Fig. 2I, Table 1). Because some *tm252* animals had no M-derived CCs (32%, *n*=115), it is possible that the *tm252* mutation also causes cell fate transformation in the M lineage.

In order to gain insight into the nature of the *tm252* mutation, we examined the localization of the mutant MLS-2 protein in *tm252* animals. Antibody staining showed that the mutant MLS-2 protein in *tm252* animals was stably made in both the M lineage (Fig. 5K,L) and the head neurons (data not shown), identical to that of wild-type MLS-2 protein. However, the mutant MLS-2 protein perdured longer and was still detectable at the 16-M stage in *tm252* mutants (Fig. 5K,L), unlike wild-type MLS-2, which is absent at this stage. Perdurance of the mutant protein was also detected in head neurons in *tm252* larvae (data not shown). This perdurance appeared to be transient, as we did not detect any mutant MLS-2 protein in the SM lineage and the signal in the additional neurons eventually faded away at the L2 larval stage (data not shown).

Several lines of evidence showed that *tm252* behaved as a semi-dominant, gain-of-function allele. First, *tm252/+* animals exhibited similar, although less severe, M lineage defects compared with *tm252/tm252* animals (Table 1). Second, as described above, the mutant MLS-2 protein in *tm252/tm252* animals perdured longer after the 8-M stage in the M lineage (Fig. 5K,L). Finally, removal of the mutant MLS-2 protein in *tm252/tm252* animals by *mls-2(RNAi)* led to abnormal division orientations, reduced cell proliferation and complete loss of CC fates, phenocopying the M lineage phenotypes of *cc615* mutants.

Mis- and overexpression of *mls-2* cause a variety of defects in the M lineage

Since loss or gain of *mls-2* function caused proliferation defects in the M lineage, we next examined the consequences of mis- and overexpression of *mls-2* inside and outside of the M lineage. We introduced a heat-shock inducible *hsp::mls-2* transgene (pYJ62) into the strain LW0081 (see Materials and methods). We then applied heat shock at various stages of larval development and examined the consequences. As expected, anti-MLS-2 antibody staining revealed high levels and global expression of MLS-2 in these transgenic animals after heat shock (data not shown).

Endogenous *mls-2* expression was detected in the M lineage from 1-M to 8-M stages. When heat shocked during these stages, a small fraction of transgenic animals died as larvae (data not shown). The remaining animals developed to fertile adults, but with various M lineage defects, including randomized cleavage orientations, increased cell proliferation and abnormal numbers of CCs and SMs (Table 2). Thus, the level of *mls-2* gene product in the M lineage is critical for its proper development.

Endogenous *mls-2* expression was not detected in the SMs or their descendants. When transgenic animals were heat shocked during 2-SM (L2 stage) to 16-SM (L3 stage) stages, CC fates were not affected. By contrast, the undifferentiated SM-descendants underwent extra rounds of cell divisions, resulting in extra numbers of VM1s (Table 2). Thus, *mls-2* is sufficient to promote cell proliferation when ectopically expressed in the SM lineage.

All M lineage-derived cells are fully differentiated at late L4 and adult stages. When heat shock was applied to transgenic animals at these stages, no M lineage defects were observed, suggesting that forced expression of *mls-2* in differentiated cells of the M lineage had no effect.

We also subjected the transgenic animals to multiple rounds of heat-shock during larval development and examined other cell types outside of the M lineage, including intestinal cells, seam cells and cells in the vulva (see Materials and methods). Although we observed slower growth and a 10% penetrance of the Pvl phenotype in the transgenic animals, we found no evidence of increased cell proliferation in the cell types examined (data not shown).

mls-2(tm252) requires *cye-1* to promote extra cell divisions in the M lineage

To better understand the mechanism of how MLS-2 regulates cell proliferation in the M lineage, we looked for cell cycle regulators that might be involved in the hyper-proliferation in *tm252* mutants. One cell cycle regulator is CYE-1, a primary trigger of S phase (Moroy and Geisen, 2004; Fay and Han, 2000; Brodigan et al., 2003).

There are two strong loss-of-function alleles of *cye-1*, *ar95* and *eh10* (Fay and Han, 2000; Brodigan et al., 2003). We found that both alleles showed similar M lineage defects: a subset of cells generated from the first three rounds of cell divisions

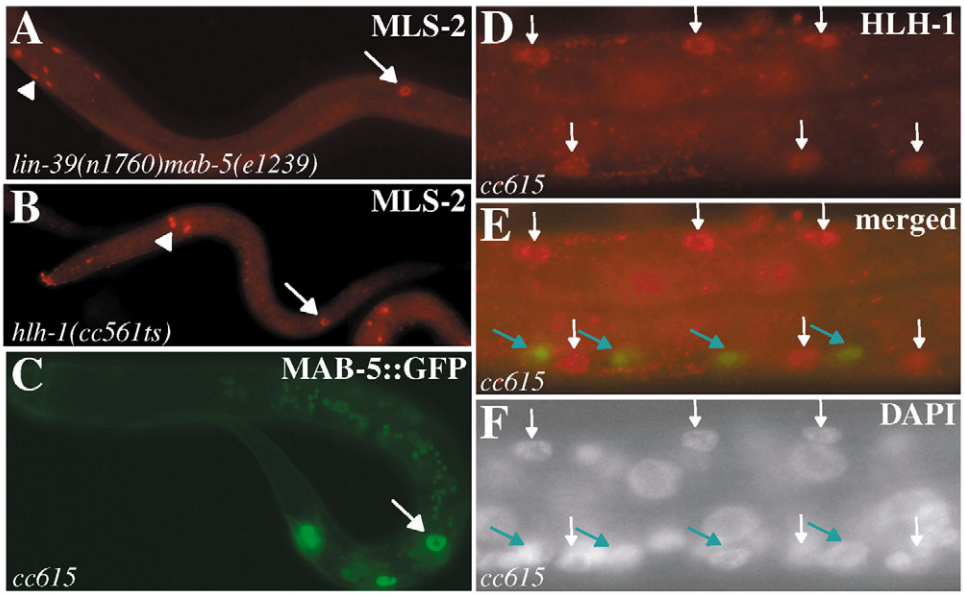

Fig. 6. *mls-2* is specifically required for the M lineage expression of *hlh-1*. (A,B) A *lin-39(n1760) mab-5(e1239)* mutant animal (A) and a *hlh-1(cc561ts)* mutant animal (B) stained with anti-MLS-2 antibodies, showing *mls-2* expression in M (arrow) and in six head neurons (arrowhead). (C) M lineage expression (arrow) of *mab-5::gfp* in a *cc615* mutant animal. (D-F) A *mls-2(cc615) ayIs6(hlh-8::gfp)* mutant animal at the 4-M stage stained with anti-HLH-1 antibodies (red in D,E) and DAPI (F). Note that HLH-1 was present in the embryonic BWMs (white arrows in D-F), but not in the four M granddaughter cells (blue arrows in E-F).

failed to divide for a fourth time, and one or both M-derived CCs were missing (Table 1). Similar to the findings of Brodigan et al. (Brodigan et al., 2003), most *cye-1* mutant animals contained two SMs (~95%, *n*>100), and the SMs exhibited variable division patterns ranging from no division to the wild-type number of divisions. A subset of the SM descendants differentiated into cells expressing *egl-15::gfp* (Table 1).

Because both *cye-1(eh10)* and *mls-2(cc615)* mutants exhibited reduced proliferation during the fourth round of cell division in the M lineage, we investigated the relationship between *cye-1* and *mls-2*. Using a *cye-1::gfp* reporter (Brodigan et al., 2003), we observed *cye-1::gfp* expression in wild-type, *cc615* and *tm252* animals throughout the early M lineage, suggesting that *mls-2* does not regulate the zygotic transcription of *cye-1*. However, lack of CYE-1 activity suppressed the hyperplasia of *tm252* mutants in the M lineage: *cye-1(eh10); mls-2(tm252)* double mutants failed to divide excessively and had one or two M-derived CCs, resembling the *cye-1(eh10)* single mutants (Table 1). This indicates that CYE-1 activity is required for the hyper-proliferative defects associated with *tm252*.

HLH-1 is a downstream target of MLS-2 in regulating cell fate specification

In addition to reduced cell proliferation, *cc615* mutants exhibited randomized cleavage orientation and cell fate transformation from CCs and BWMs to SMs in the M lineage. Several previously described mutants share similar M lineage defects. *mab-5(e1239)* and *hlh-8(nr2061)* mutants show abnormal cleavage orientation in the M lineage, whereas *mab-5(e1239)* and *hlh-1(cc561ts)* exhibit fate transformation from CCs to SMs (Kenyon, 1986; Harfe et al., 1998a; Harfe et al., 1998b; Corsi et al., 2000; Corsi et al., 2002). Both *mab-5* (encoding a Hox factor) and *hlh-8* (encoding CeTwist) are expressed in the early M lineage, with *hlh-8* being a direct target of *mab-5* and *lin-39* (S. J. Salser, PhD thesis, University of California, San Francisco, 1995) (Harfe et al., 1998b; Liu and Fire, 2000). *hlh-1* encodes CeMyoD and is expressed in both the embryonic and M-derived BWMs, as well as in the early M lineage from the 2-M stage to 16-M stage, prior to differentiation (Krause et al., 1990; Harfe et al., 1998a).

We investigated the regulatory relationship between *mls-2* and *mab-5*, and *hlh-8* and *hlh-1*. Normal levels and patterns of MLS-2 expression were detected by anti-MLS-2 antibodies in *lin-39(n1760) mab-5(e1239)*, *hlh-8(nr2061)* and *hlh-1(cc561ts)* mutants at the non-permissive temperature (Fig. 6A,B, data not shown). Similarly, expression of *mab-5::gfp* and *hlh-8::gfp* was detected in the M lineage of *cc615* mutants (Fig. 2B-H, Fig. 6C). By contrast, the M lineage-specific expression of HLH-1 was not detectable by anti-HLH-1 antibodies in *cc615* mutants, even though the same animals showed positive staining of HLH-1 in the embryonic BWMs (Fig. 6D-F). These results suggest that the M lineage expression of *hlh-1* requires MLS-2 activity. Consistent with this, *hlh-1(RNAi)* in *cc615* mutants did not produce any additional phenotypes in the M lineage. Furthermore, *hlh-1(cc561ts); mls-2(tm252)* double mutants completely lacked M-derived CCs (data not shown), resembling the phenotype of *hlh-1(cc561ts)* single mutants. Additional cell proliferation in the M lineage was still detected in the *hlh-1(cc561ts); mls-2(tm252)* double mutants, indicating that HLH-1 is not required for MLS-2 function in cell proliferation. Thus MLS-2 acts through HLH-1 to regulate coelomocyte fate specification in the M lineage. Forced expression of *hlh-1* in the M lineage could not rescue the loss of CC fates in *cc615* mutants (data not shown), suggesting that at least one other target of MLS-2 exists in regulating CC fate specification in the M lineage.

Discussion

MLS-2 is both necessary and sufficient to promote cell proliferation in the M lineage

We have shown that loss of MLS-2 function in *cc615* mutants resulted in reduced proliferation during the fourth round of cell division, whereas a gain-of-function allele, *tm252*, caused increased proliferation in the M lineage (Fig. 2). In addition,

forced expression of *mls-2* in wild-type animals, using either the *hlh-8* promoter (data not shown) or the heat-shock promoter (Table 2), resulted in over-proliferation in the M lineage. Thus MLS-2 is both necessary and sufficient for promoting cell proliferation in the M lineage. The ability of MLS-2 to promote cell proliferation appears to be limited to the M lineage. Although forced expression of *mls-2* caused over-proliferation in the early M lineage and the SM lineage, we did not observe any over-proliferation in the examined cell types outside of the M lineage. This suggests that other co-factor(s) specifically expressed in the M lineage might be required for MLS-2 to function in regulating cell proliferation.

Previous studies have shown that the G1 cyclin CYE-1 is present in many postembryonic blast cells, and is required for vulval and M lineage development (Fay and Han, 2000; Brodigan et al., 2003). Fay and Han (Fay and Han, 2000) have also reported that only the last rounds of cell divisions during vulval development are affected in *cye-1* mutants. Consistent with their findings, we observed that *cye-1(eh10)* mutants exhibited proliferation defects only after the first three rounds of cell divisions in the M lineage, suggesting that maternal CYE-1 is sufficient for those cell divisions. Because *mls-2(cc615)* mutants and *cye-1(eh10)* mutants showed very similar proliferation defects, MLS-2 may be required to regulate either the expression or the activity/stability of CYE-1. We found that zygotic expression of *cye-1* was not affected in *cc615* mutants. However, a *cye-1* null mutation, *cye-1(eh10)*, suppressed the over-proliferation defects of *mls-2(tm252)* mutants. Thus MLS-2 might regulate the stability and/or activity of CYE-1 in the M lineage.

MLS-2 controls cell fate specification through HLH-1 in the M lineage

In addition to regulating cell proliferation, MLS-2 also plays a role in regulating cell fate specification. *mls-2(cc615)* mutants exhibit cell fate transformation from BWMs and CCs to SMs, suggesting that MLS-2 function is required for the CC and BWM fates. One of the known factors required for these fates is the *C. elegans* Myod homolog HLH-1 (Harfe et al., 1998a). Our data suggest that HLH-1 is a specific target of MLS-2 in regulating cell fate specification. We have found that HLH-1 is not present in the M lineage in *cc615* mutants (Fig. 6), and that reducing HLH-1 activity in *tm252* mutants suppresses the CC cell fate without affecting the hyper-proliferation defects. Currently it is not clear whether *hlh-1* is a direct target of MLS-2 and whether other targets of MLS-2 also exist in regulating cell fate specification in the M lineage.

MLS-2 has multiple and distinct functions in regulating cleavage orientation, cell proliferation and cell fate specification

MLS-2 is a cell type-specific homeodomain protein that regulates cleavage orientation, cell proliferation and fate specification in the M lineage. Several lines of evidence support the model that MLS-2 exerts its multiple functions through distinct mechanisms. First, the gain-of-function *tm252* mutants only exhibited defects in cell proliferation and fate specification without affecting cleavage orientation, suggesting that the function of MLS-2 in regulating cleavage orientation can be uncoupled from its other functions. Second, lack of CYE-1 activity specifically suppressed the hyper-proliferation defects of *tm252* mutants, whereas removal of HLH-1 activity specifically affected CC fate specification. These results suggest that MLS-2 has distinct sets of downstream target genes regulating cell proliferation and cell fate specification.

Previous studies in a number of systems have shown that cell fate specification is tightly coupled to cell division and cell cycle progression (Cremisi et al., 2003; Malicki, 2004). In particular, progression through the cell cycle is required for the expression of cell fate determinants, as shown in the fly nervous system (Weigmann and Lehner, 1995) and the *C. elegans* vulval precursor cells (Ambros, 1999). We failed to detect HLH-1 expression even in proliferating cells in the M lineage of *mls-2(cc615)* mutants, suggesting that the expression of HLH-1 was not dependent on cell cycle progression in the M lineage. At this point, we cannot rule out the possibility that other cell fate determinant(s) are not expressed in *mls-2(cc615)* mutants because of reduced cell proliferation.

Developmental control of MLS-2 activity and coordination between cell proliferation and differentiation

Our studies suggest that *mls-2* expression can be regulated at both the transcriptional level and the post-transcriptional level. At the transcriptional level, the *mls-2* promoter is specifically active in the early M lineage (1-M to 16-M stage). At the post-transcriptional level, MLS-2 protein can only be detected up to the 8-M stage (Fig. 5). Interestingly, it is at the 16-M stage when most M-derived cells exit the cell cycle and become differentiated (Fig. 1). Because mutants lacking MLS-2 fail to undergo the fourth round of cell division after the 8-M stage, MLS-2 needs to be present in the eight proliferating M lineage descendants to allow them to divide. Once these cells divide, MLS-2 activity needs to be promptly removed to allow these cells to exit the cell cycle and differentiate. Consistent with this, we observed excessive proliferation in *tm252* mutants where the mutant MLS-2 protein perdured beyond the 8-M stage. Thus MLS-2 appears to be a pro-proliferation and/or anti-differentiation factor whose activity needs to be tightly regulated to allow the transition from cell proliferation to differentiation. Because the *tm252* allele deletes the entire exon 3 and part of exon 4, those regions may contain the regulatory element(s) that are required for regulating the stability of the MLS-2 protein.

The HMX protein family: conserved and divergent sequences and functions

HMX family of homeodomain proteins shares a highly conserved homeodomain and two additional conserved regions located immediately C-terminal to the homeodomain (Fig. 4). These two additional regions do not appear to be conserved in MLS-2 and the chick protein SOHo1 (Deitcher et al., 1994) (Fig. 4). Outside of these conserved regions, sequences are highly diverged among the HMX family members.

Previous studies have shown that the vertebrate and the *Drosophila* HMX proteins share a common expression in the nervous system, with the vertebrate HMX proteins also being expressed in a number of sensory organs (Adamska et al., 2000; Adamska et al., 2001; Bober et al., 1994; Deitcher et al., 1994; Hadrys et al., 1998; Herbrand et al., 1998; Kiernan et al., 1997; Rinkwitz-Brandt et al., 1995; Rinkwitz-Brandt et al.,

1996; Stadler et al., 1995; Stadler and Solursh, 1994; Wang et al., 1990; Wang et al., 1998; Wang et al., 2000; Yoshiura et al., 1998; Adamska et al., 2001). Mice lacking either *Hmx2* or *Hmx3*, or both, have various defects in the CNS and the inner ear (Wang et al., 1998; Wang et al., 2001; Wang et al., 2004). Significantly, *Drosophila Hmx* can rescue the CNS defects, as well as the inner ear defects, of the *Hmx2; Hmx3* double knockout mice (Wang et al., 2004). These observations suggest a conserved function of the HMX proteins in the nervous system. We have also observed neuronal expression of *mls-2* (Fig. 5). Thus, MLS-2 might share with other HMX family members their conserved functions in the nervous system.

We have found that MLS-2 plays crucial roles in the development of the postembryonic mesoderm in *C. elegans*. Expression of HMX proteins outside of the nervous system and the sensory organs has been reported, and mice lacking *Hmx3* show inner ear defects and maternal reproductive defects (Martinez and Davidson, 1997; Shaw et al., 2003; Stadler and Solursh, 1994; Wang et al., 1998). Therefore, like *mls-2*, the *Hmx* genes in other organisms might also be expressed and functioning in additional cell types, especially during postembryonic development.

We have shown that MLS-2 is required for cell proliferation and fate specification in the M lineage. Mice that lack *Hmx2*, or both *Hmx2* and *Hmx3*, exhibit reduced proliferation in the otic epithelium and the adjacent mesenchyme, as well as alteration of cell fates in the otic vesicle (Wang et al., 2001; Wang et al., 2004). Interestingly, although *Drosophila Hmx* can functionally replace *Hmx2* and *Hmx3* in the murine inner ear and hypothalamus, it appears to be more effective in rescuing the decreased cell proliferation defects of the *Hmx2; Hmx3* double mutants (Wang et al., 2004). We therefore propose that one of the most conserved functions of HMX proteins is to regulate cell proliferation. We have identified one cell cycle regulator, CYE-1, whose activity/stability is regulated by MLS-2. Future studies of HMX proteins in other systems will shed light on whether this and other functions of MLS-2 are conserved for all HMX proteins.

We thank Ann Corsi, Alan Coulson, Andy Fire, Mike Krause, Yuji Kohara and Shohei Mitani for *C. elegans* strains, cosmids, cDNA clones and antibodies; Alexander Soneru for performing the egg-laying assays; Ann Corsi, Andy Fire, Ken Kemphues, Mike Krause, Sylvia Lee, Diane Morton, Qi Sun, Mariana Wolfner and members of the Liu lab for helpful discussions, suggestions and valuable comments on the manuscript. We also thank two anonymous reviewers for valuable suggestions on the manuscript. J.L. appreciates the advice and support of Andy Fire, in whose lab the *mls-2(cc615)* mutant was isolated. Some strains used in this study were obtained from the *C. elegans* Genetics Center (CGC), which is supported by a grant from the NIH National Center for Research Resources. This work is supported by NIH R01 GM066953 (to J.L.).

References

Adamska, M., Leger, S., Brand, M., Hadrys, T., Braun, T. and Bober, E. (2000). Inner ear and lateral line expression of a zebrafish Nkx5-1 gene and its downregulation in the ears of FGF8 mutant ace. *Mech Dev*. **97**, 161-165.

Adamska, M., Wolff, A., Kreusler, M., Wittbrodt, J., Braun, T. and Bober, E. (2001). Five Nkx5 genes show differential expression patterns in anlagen of sensory organs in medaka: insight into the evolution of the gene family. *Dev. Genes Evol*. **211**, 338-349.

Ambros, V. (1999). Cell cycle-dependent sequencing of cell fate decisions in *Caenorhabditis elegans* vulva precursor cells. *Development* **126**, 1947-1956.

Bober, E., Baum, C., Braun, T. and Arnold, H. H. (1994). A novel NK related mouse homeobox gene: expression in central and peripheral nervous structures during embryonic development. *Dev. Biol*. **162**, 288-303.

Brenner, S. (1974). The genetics of *Caenorhabditis elegans*. *Genetics* **77**, 71-94.

Brodigan, T. M., Liu, J., Park, M., Kipreos, E. T. and Krause, M. (2003). Cyclin E expression during development in *Caenorhabditis elegans*. *Dev. Biol*. **254**, 102-115.

Burdine, R. D., Branda, C. S. and Stern, M. J. (1998). EGL-17(FGF) expression coordinates the attraction of the migrating sex myoblasts with vulval induction in *C. elegans*. *Development* **125**, 1083-1093.

Corsi, A. K., Kostas, S. A., Fire, A. and Krause, M. (2000). *Caenorhabditis elegans* Twist plays an essential role in non-striated muscle development. *Development* **127**, 2041-2051.

Corsi, A. K., Brodigan, T. M., Jorgensen, E. M. and Krause, M. (2002). Characterization of a dominant negative *C. elegans* Twist mutant protein with implications for human Saethre-Chotzen syndrome. *Development* **129**, 2761-2772.

Cremisi, F., Philpott, A. and Ohnuma, S. (2003). Cell cycle and cell fate interactions in neural development. *Curr. Opin. Neurobiol*. **13**, 26-33.

Deitcher, D. L., Fekete, D. M. and Cepko, C. L. (1994). Asymmetric expression of a novel homeobox gene in vertebrate sensory organs. *J. Neurosci.* **14**, 486-498.

Fay, D. S. and Han, M. (2000). Mutations in *cye-1*, a *Caenorhabditis elegans* cyclin E homolog, reveal coordination between cell-cycle control and vulval development. *Development* **127**, 4049-4060.

Fire, A., Xu, S., Montgomery, M. K., Kostas, S. A., Driver, S. E. and Mello, C. C. (1998). Potent and specific genetic interference by double-stranded RNA in *Caenorhabditis elegans*. *Nature* **391**, 806-811.

Granato, M., Schnabel, H. and Schnabel, R. (1994). *pha-1* a selectable marker for gene transfer in *C. elegans*. *Nucleic Acids Res*. **22**, 1762-1763.

Greenwald, I. S., Sternberg, P. W. and Horvitz, H. R. (1983). The *lin-12* locus specifies cell fates in *Caenorhabditis elegans*. *Cell* **34**, 435-444.

Hadrys, T., Braun, T., Rinkwitz-Brandt, S., Arnold, H. H. and Bober, E. (1998). Nkx5-1 controls semicircular canal formation in the mouse inner ear. *Development* **125**, 33-39.

Harfe, B. D., Branda, C. S., Krause, M., Stern, M. J. and Fire, A. (1998a). MyoD and the specification of muscle and non-muscle fates during postembryonic development of the *C. elegans* mesoderm. *Development* **125**, 2479-2488.

Harfe, B. D., Gomes, A. V., Kenyon, C., Liu, J., Krause, M. and Fire, A. (1998b). Analysis of a *Caenorhabditis elegans* Twist homolog identifies conserved and divergent aspects of mesodermal patterning. *Genes Dev.* **12**, 2623-2635.

Hecht, R. M., Norman, M. A., Vu, T. and Jones, W. (1996). A novel set of uncoordinated mutants in *Caenorhabditis elegans* uncovered by cold-sensitive mutations. *Genome* **39**, 459-464.

Herbrand, H., Guthrie, S., Hadrys, T., Hoffmann, S., Arnold, H. H., Rinkwitz-Brandt, S. and Bober, E. (1998). Two regulatory genes, cNkx5-1 and cPax2, show different responses to local signals during otic placode and vesicle formation in the chick embryo. *Development* **125**, 645-654.

Hodgkin, J. A., Horvitz, H. R. and Brenner, S. (1979). Nondisjunction mutants of the nematode *C. elegans*. *Genetics* **91**, 67-94.

Hurd, D. D. and Kemphues, K. J. (2003). PAR-1 is required for morphogenesis of the *Caenorhabditis elegans* vulva. *Dev. Biol*. **253**, 54-65.

Kenyon, C. (1986). A gene involved in the development of the posterior body region of *C. elegans*. *Cell* **46**, 477-487.

Kiernan, A. E., Nunes, F., Wu, D. K. and Fekete, D. M. (1997). The expression domain of two related homeobox genes defines a compartment in the chicken inner ear that may be involved in semicircular canal formation. *Dev Biol*. **191**, 215-229.

Kostas, S. A. and Fire, A. (2002). The T-box factor MLS-1 acts as a molecular switch during specification of nonstriated muscle in *C. elegans*. *Genes Dev*. **16**, 257-269.

Krause, M., Fire, A., Harrison, S. W., Priess, J. and Weintraub, H. (1990). CeMyoD accumulation defines the body wall muscle cell fate during *C. elegans* embryogenesis. *Cell* **63**, 907-919.

Liu, J. and Fire, A. (2000). Overlapping roles of two Hox genes and the *exd* ortholog *ceh-20* in diversification of the *C. elegans* postembryonic mesoderm. *Development* **127**, 5179-5190.

Malicki, J. (2004). Cell fate decisions and patterning in the vertebrate retina: the importance of timing, asymmetry, polarity and waves. *Curr. Opin. Neurobiol*. **14**, 15-21.

Maloof, J. N. and Kenyon, C. (1998). The Hox gene *lin-39* is required during

C. elegans vulval induction to select the outcome of Ras signaling. *Development* **125**, 181-190.

Martinez, P. and Davidson, E. H. (1997). *SpHmx*, a sea urchin homeobox gene expressed in embryonic pigment cells. *Dev. Biol.* **181**, 213-222.

Mello, C. C., Kramer, J. M., Stinchcomb, D. and Ambros, V. (1991). Efficient gene transfer in *C. elegans*: extrachromosomal maintenance and integration of transforming sequences. *EMBO J.* **10**, 3959-3970.

Moroy, T. and Geisen, C. (2004). Cyclin E. *Int. J. Biochem. Cell Biol.* **36**, 1424-1439.

Okkema, P. G. and Fire, A. (1994). The *Caenorhabditis elegans* NK-2 class homeoprotein CEH-22 is involved in combinatorial activation of gene expression in pharyngeal muscle. *Development* **120**, 2175-2186.

Page, R. D. (1996). TreeView: an application to display phylogenetic trees on personal computers. *Comput. Appl. Biosci.* **12**, 357-358.

Pollard, S. L. and Holland, P. W. (2000). Evidence for 14 homeobox gene clusters in human genome ancestry. *Curr. Biol.* **10**, 1059-1062.

Rinkwitz-Brandt, S., Justus, M., Oldenettel, I., Arnold, H. H. and Bober, E. (1995). Distinct temporal expression of mouse *Nkx-5.1* and *Nkx-5.2* homeobox genes during brain and ear development. *Mech. Dev.* **52**, 371-381.

Rinkwitz-Brandt, S., Arnold, H. H. and Bober, E. (1996). Regionalized expression of *Nkx5-1, Nkx5-2, Pax2* and *sek* genes during mouse inner ear development. *Hear. Res.* **99**, 129-138.

Seydoux, G., Savage, C. and Greenwald, I. (1993). Isolation and characterization of mutations causing abnormal eversion of the vulva in Caenorhabditis elegans. *Dev. Biol.* **157**, 423-436.

Schnabel, H. and Schnabel, R. (1990). An organ-specific differentiation gene, *pha-1*, from *C. elegans*. *Science* **250**, 686-688.

Shaw, P. A., Zhang, X., Russo, A. F., Amendt, B. A., Henderson, S. and Williams, V. (2003). Homeobox protein, Hmx3, in postnatally developing rat submandibular glands. *J. Histochem. Cytochem.* **51**, 385-396.

Smith, D. B. and Johnson, K. S. (1988). Single-step purification of polypeptides expressed in *Escherichia coli* as fusions with glutathione S-transferase. *Gene* **67**, 31-40.

Stadler, H. S. and Solursh, M. (1994). Characterization of the homeoboxcontaining gene *GH6* identifies novel regions of homeobox gene expression in the developing chick embryo. *Dev. Biol.* **161**, 251-262.

Stadler, H. S., Padanilam, B. J., Buetow, K., Murray, J. C. and Solursh, M. (1992). Identification and genetic mapping of a homeobox gene to the 4p16.1 region of human chromosome 4. *Proc. Natl. Acad. Sci. USA* **89**, 11579-11583.

Stadler, H. S., Murray, J. C., Leysens, N. J., Goodfellow, P. J. and Solursh, M. (1995). Phylogenetic conservation and physical mapping of members of the *H6* homeobox gene family. *Mamm. Genome* **6**, 383-388.

Sulston, J. E. and Horvitz, H. R. (1977). Post-embryonic lineages of the nematode *Caenorhabditis elegans*. *Dev. Biol.* **56**, 110-156.

Sulston, J. E., Schierenberg, E., White, J. G. and Thomas, J. N. (1983). The embryonic cell lineage of the nematode *Caenorhabditis elegans*. *Dev. Biol.* **100**, 64-119.

Wang, G. V. L., Dolecki, G. J., Carlos, R. and Humphreys, T. (1990). Characterization and expression of two sea urchin homeobox sequences. *Dev. Genet.* **11**, 77-87.

Wang, S. and Kimble, J. (2001). The TRA-1 transcription factor binds TRA-2 to regulate sexual fates in *Caenorhabditis elegans*. *EMBO J.* **20**, 1363-1372.

Wang, W., Van De Water, T. and Lufkin, T. (1998). Inner ear and maternal reproductive defects in mice lacking the Hmx3 homeobox gene. *Development* **125**, 621-634.

Wang, W., Lo, P., Frasch, M. and Lufkin, T. (2000). Hmx: an evolutionary conserved homeobox gene family expressed in the developing nervous system in mice and Drosophila. *Mech. Dev.* **99**, 123-137.

Wang, W., Chan, E. K., Baron, S., Van de Water, T. and Lufkin, T. (2001). Hmx2 homeobox gene control of murine vestibular morphogenesis. *Development* **128**, 5017-5029.

Wang, W., Grimmer, J. F., Van De Water, T. and Lufkin, T. (2004). Hmx2 and Hmx3 homeobox genes direct development of the murine inner ear and hypothalamus and can be functionally replaced by Drosophila Hmx. *Dev. Cell* **7**, 439-453.

Weigmann, K. and Lehner, C. F. (1995). Cell fate specification by even-skipped expression in the *Drosophila* nervous system is coupled to cell cycle progression. *Development* **121**, 3713-3721.

Wicks, S. R., Yeh, R. T., Gish, W. R., Waterston, R. H. and Plasterk, R. H. (2001). Rapid gene mapping in *Caenorhabditis elegans* using a high density polymorphism map. *Nat. Genet.* **28**, 160-164.

Yoshiura, K., Leysens, N. J., Reiter, R. and Murray, J. C. (1998). Cloning, characterization, and mapping of the mouse homeobox gene Hmx1. *Genomics* **50**, 61-68.